

Maximum likelihood bolometric tomography for the determination of the uncertainties in the radiation emission on JET TOKAMAK

*Original*

Maximum likelihood bolometric tomography for the determination of the uncertainties in the radiation emission on JET TOKAMAK / Craciunescu, Teddy; Peluso, Emmanuele; Murari, Andrea; Gelfusa, Michela; Subba, F.. - In: REVIEW OF SCIENTIFIC INSTRUMENTS. - ISSN 0034-6748. - 89:5(2018). [10.1063/1.5027880]

*Availability:*

This version is available at: 11583/2986825 since: 2024-03-11T18:28:24Z

*Publisher:*

AMER INST PHYSICS

*Published*

DOI:10.1063/1.5027880

*Terms of use:*

This article is made available under terms and conditions as specified in the corresponding bibliographic description in the repository

*Publisher copyright*

AIP postprint/Author's Accepted Manuscript e postprint versione editoriale/Version of Record

(Article begins on next page)

# Maximum Likelihood Bolometric Tomography for the Determination of the Uncertainties in the Radiation Emission on JET

Teddy Craciunescu<sup>a</sup>, Emmanuele Peluso<sup>b</sup>, Andrea Murari<sup>c</sup> and Michela Gelfusa<sup>b</sup>  
and JET Contributors<sup>§</sup>

*EUROfusion Consortium, JET, Culham Science Centre, Abingdon, OX14 3DB, UK*

*<sup>a</sup>National Institute for Laser, Plasma and Radiation Physics, Magurele-Bucharest, Romania,*

*<sup>b</sup>University of Rome "Tor Vergata", Roma, Italy*

*<sup>c</sup>Consorzio RFX, Padova, Italy*

§ See the author list of "X. Litaudon et al 2017 Nucl. Fusion 57 102001

## Abstract

The total emission of radiation is a crucial quantity to calculate the power balances and to understand the physics of any Tokamak. Bolometric systems are the main tool to measure this important physical quantity through quite sophisticated tomographic inversion methods. On JET, the coverage of the bolometric diagnostic, due to the availability of basically only two projection angles, is quite limited, rendering the inversion a very ill-posed mathematical problem. A new approach, based on the maximum likelihood, has therefore been developed and implemented, to alleviate one of the major weaknesses of traditional tomographic techniques: the difficulty to determine routinely the confidence intervals in the results. The method has been validated by numerical simulations with phantoms, to assess the quality of the results and to optimise the configuration of the parameters, for the main types of emissivity encountered experimentally. The typical levels of statistical errors, which may significantly influence the quality of the reconstructions, have been identified. The systematic tests with phantoms indicate that the errors in the reconstructions are quite limited and their effect on the total radiated power remains well below 10%. A comparison with other approaches to the inversion and to the regularization has also been performed.

**Keywords:** Tokamaks, power balances, uncertainty assessment, reconstruction artefacts, bolometry, tomography, radiation emission, maximum likelihood.

## 1. Total Radiated power and Bolometry

In Tokamaks, the total radiation emission is a very important quantity to measure [1]. This is particularly true in metallic machines, whose performance can be strongly affected by the transport of heavy impurities and the consequent radiation patterns. The diagnostic typically used to measure the emitted radiation is bolometry. On JET, given the layout of the diagnostic reported in Figure 1, the tomographic inversion of the bolometric signals is a very ill-posed problem. The system comprises two cameras with horizontal and vertical views across the cross-section of the plasma. 24 chords are available for each view [2]. Their geometry allows an increased spatial resolution in the divertor region. The availability of only two views (projections

in tomographic language) leads to a quite limited data set tomographic problem. Therefore, to determine both the total radiated power and the local emissivity, quite sophisticated tomographic inversion methods are required. Special algorithms, specific to the machine and to its constraints and allowing effective tomography from the available limited data, are needed. In the course of the years, various tomographic methods have been tested [3-5]. Tomographic reconstruction is currently performed with the method originally developed by Ingesson [3]. It is based on a grid of pyramid local basis functions that are used for the discretization of the tomographic problem. The algorithm searches for a solution, which is constant on flux surface and gently varying in the radial direction. Recently a new approach,

based on deep neural networks, trained on an ensemble of measurements and reconstructions obtained using the method described in [3], has been proposed [4]. In case of a successful training, able to robustly generalize the knowledge in the training data, the method has the potential of providing fast reconstructions, allowing the processing of a large amount of data. The idea of using neural networks for the determination of radiated power in JET has been proposed for the first time in [5]. In this approach, besides the bolometric data, elongation and triangularity were used as input to the neural network, since these provide useful complementary information. The method is also applicable in real-time without any major difficulty. However, the problem of estimating the errors associated with the reconstructed emissivity profile is still open. Accurate modelling of the projection noise propagation is important for both qualitative interpretation and quantitative analysis of the reconstructed images. The Monte Carlo approaches do not represent a solution because repeated measurements with multiple noise realizations cannot be achieved experimentally. Therefore, analytic solutions, applicable on a routine basis, would be very advantageous. Unfortunately, the class of methods successfully applied in JET are highly non-linear algorithms, many of them relying on iterative reconstruction schemes, which can accommodate implicit or explicit models of the image formation process. The non-linearities of these algorithms render much more difficult the full description of the final image and error statistics.

In the present paper, we propose to apply to bolometry a reconstruction method based on the statistical Maximum Likelihood (ML) principle, which has been successfully used for gamma and neutron tomography in JET [6-7]. The complementary implementation of the recently developed methodology for the numerical evaluation of the reconstruction uncertainties [8] allows estimating the error bars, when deriving the total radiated power and the power profiles from bolometry. Indeed, among the tomographic approaches, which can be considered good candidate for JET bolometric tomography, the ML technique can take advantage of this existing methodological background and experience, particularly to address the issue of estimating the uncertainties in the final reconstructions. To this end, the same approach has also already been used on JET for the gamma and neutron topographies, which, on the other hand, have completely different diagnostic layouts and emissivity shapes and therefore constitute different mathematical problems.

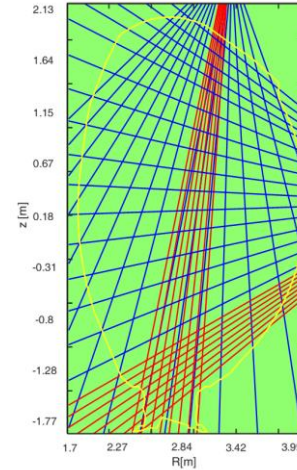


Figure 1 – Schematic view of JET bolometric diagnostic layout.

Over the last two decades, different new approaches dedicated to reconstruction uncertainty estimation have emerged. In the early nineties, Barrett et al derived approximate formulae for the ensemble mean and covariance of the ML expectation maximization reconstruction [9]. This approach has been extended to one-step-late [10] and later to block iterative algorithms [11-12]. Qi [13] proposed a unified noise analysis for the iterative reconstruction algorithms based on the gradient ascent update formulas. An alternative approach has been promoted by Fessler [14], who proposed a method, which can analyze the mean and variance of reconstructed images at the fixed point of the objective function. The properties of noise and different noise metrics have been studied for various kinds of tomography setups (see e.g. Refs. 15-17). The refinements of the tomographic inversion based on the Maximum Likelihood, presented in this paper, profit from these recent developments in the reconstruction techniques (see next sections).

The present paper is organized as follows: the next section is a review of the ML tomographic method, particularised for the case of JET bolometric diagnostic. Section 3 is devoted to the procedure for deriving the statistical properties of the reconstructed emission, to quantify the uncertainties in the inversion. The overall quality of the method has been assessed with phantoms, as described in Section 4 for experimental cases of emissivity. The results obtained applying the ML tomographic technique to JET experimental data are reported in Section 5. Conclusions and the potential additional applications of the methodology are drawn in the last section of the paper.

## 2 The Maximum Likelihood Tomographic Method

From a mathematical point of view, the tomographic reconstruction of 2-D emission from projections can be formulated as:

$$\bar{g}_m = \sum_{n=1}^{N_p} H_{mn} \bar{f}_n, \quad m = 1, \dots, N_d \quad (1)$$

where:

- $\bar{g}_m$  is the mean number of photons detected in the projection bin  $m$ :

$$g = \bar{g} + n_g \quad (2)$$

where  $g$  and  $n_g$  are the experimental measurement and the accompanying zero-mean noise, respectively.

- $\bar{f}_n$  denotes the expected emissivity distribution over all noisy realizations of the mean data  $\bar{g}_m$

$$f = \bar{f} + n_f \quad (3)$$

where  $n_f$  is the zero mean image noise vector.

- $N_p$  is the total number of pixels and  $N_d$  is the total number of detectors.

The measurements are integrals over the emissivity distribution taken along physically well defined lines of sight. The projection matrix element  $H_{mn}$  represents the probability of detecting in detector  $m$  emission from pixel  $n$ . The tomographic equation can be re-written in matrix form:

$$g = Hf + n_g \quad (4)$$

The emission is considered a Poisson process and therefore  $g_m$  is a sample from a Poisson distribution, whose expected value is  $\bar{g}$ . Consequently, the probability of obtaining the measurement  $g = \{g_m | m = 1, \dots, N_d\}$  from the emissivity  $f = \{f_n | n = 1, \dots, N_p\}$  is given by the likelihood function:

$$L(g/f) = \prod_m \frac{1}{g_m!} (\bar{g})^{g_m} \times \exp(-\bar{g}) \quad (5)$$

The ML estimate is obtained by maximizing the above expression:

$$f_{ML} = \operatorname{argmax}_f L(g|f) \quad (6)$$

An iterative solution has been proposed by Lange and Carson [18]:

$$f_n^{(k+1)} = \frac{f_n^{(k)}}{s_n} \sum_m (g_m / \sum_j H_{mj} f_j^{(k)}) H_{mn} \quad (7)$$

where  $k$  is indexing the iterations and  $s_n = \sum_m H_{mn}$  is the probability that a photon originating in pixel  $n$  will be recorded in a projection bin.

JET bolometric tomography is a highly undetermined inversion. This, combined with the complicated shapes of the radiation emission, results in a very ill-posed mathematical problem. To obtain realistic and robust solutions, it is therefore indispensable to introduce additional a priori information, in order to compensate for the lack of experimental information. A common approach in JET implementations consists of imposing smoothness on the solutions of the tomographic problem [4]. The ML method developed for the bolometric diagnostic incorporates a regularizing procedure that assumes smoothness along the magnetic surfaces, given by the plasma equilibrium.

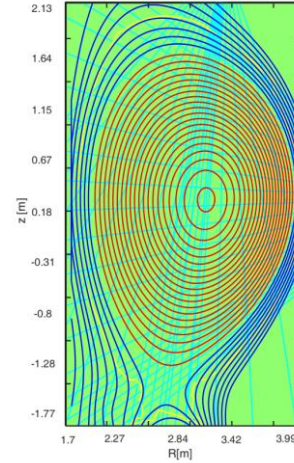


Figure 2 – Two different smoothing procedures are used for the closed (red curves) and open (blue curves) magnetic surfaces.

For the closed magnetic surfaces (Fig. 2 – red curves), the smoothing is implemented as a 1-D average filtering, using a sliding window, which moves along the magnetic contour lines [6-7]:

$$f_i^{smooth} = \frac{1}{2 \cdot w_{ave}} \sum_{j=-w_{ave}}^{w_{ave}} f_j \quad (8)$$

where  $f^{reg}$  is the image after applying the smoothing regularizing procedure,  $w_{ave}$  is equal to half of the width of the filtering window and  $L_p$  designates the  $p$ -th close magnetic contour line. For the open magnetic surfaces (Fig. 2 – blue curves), we have implemented a smoothing spline procedure, which is based on the minimisation of the expression:

$$p \sum_i (f_i^{smooth} - f_i)^2 + (1-p) \int (f_i'')^2 dx \quad (9)$$

where  $f''$  is the second derivative of  $f$  and  $p \in (0,1)$  is an adjustable parameter; for  $p = 0$  the minimization of (9) produces a least-squares straight-line fit to the data, while for  $p = 1$  produces a cubic spline interpolant.

### 3. Noise propagation in Maximum Likelihood Reconstructions

In the present work, the derivation of approximate formulae for the mean and covariance of the reconstructions is based on the general formalism developed in [13]. A preconditioned gradient ascent algorithm for solving (6) is given by the relation:

$$f^{k+1} = f^k + \alpha C^k(f^k) [\nabla_x L(g|f)]_{f=f^k} \quad (10)$$

where  $\alpha > 0$  is a fixed step size and  $C^k(f^k)$  is the preconditioner.

As we are interested in the noise accompanying the reconstructed image at each iteration  $k$ , it is convenient to re-write (2)-(3) in the form:

$$g^k = \bar{g}^k + n \quad (11)$$

$$f^k = \bar{f}^k + \varepsilon^k \quad (12)$$

The first approximation, needed for the derivation of a formula for updating  $\varepsilon^{(k)}$  at each iteration, is the assumption that the noise in the reconstruction is small compared to the mean value of the reconstruction. This approximation, first introduced in [9] and widely used in other approaches, allow the first-order Taylor expansion:

$$\nabla_x L(g|f^k) \approx \nabla_x L(\bar{g}|\bar{f}^k) + \nabla_{xx} L(\bar{g}|\bar{f}^k)n + \nabla_{xx} L(\bar{g}|\bar{f}^k)\varepsilon^k \quad (13)$$

$$C^k(f^k) \approx C^k(\bar{f}^k) + C^k(\varepsilon^k, \bar{f}^k) \quad (14)$$

Substituting (13)-(14) in (10), neglecting the second order noise terms and equating random terms to random terms and non-random ones to non-random ones, the following equations can be obtained (please see [13] for the details of these calculations):

$$f^{k+1} \approx f^k + \alpha C^k(\bar{f}^k) \nabla_x L(\bar{g}|\bar{f}^k) \quad (15)$$

$$\varepsilon^{k+1} \approx [I - A^k]V^k + B^k \quad (16)$$

where:

$$A^k = -\alpha C^k(\bar{f}^k) \nabla_x L(\bar{g}|\bar{f}^k) - \alpha M[\nabla_x L(\bar{g}|\bar{f}^k), \bar{f}^k] \quad (17)$$

$$B^k = \alpha C^k(\bar{f}^k) \nabla_{xy} L(\bar{g}|\bar{f}^k) \quad (18)$$

and where the  $(j,l)$  element of  $M[y;f]$  is  $\sum_m y_m \partial C_{j,m}^k(f) \partial f_l$ .

Eq. (15) gives a explicit multiplicative update equation for retrieving the reconstructed image  $f^k$ , at each iteration from the noise-free data, while Eq. (16) provides a rule for finding the uncertainty accompanying the current reconstruction estimate.

With regard to the correlation properties of the uncertainties, using the notation:

$$V^{k+1} = [I - A^k]V^k + B^k \quad (19)$$

and starting from (16), it can be proved that the covariance of the reconstructed image  $Cov(f)$  can be expressed in terms of the covariance of the projection data  $Cov(g)$ :

$$Cov(f) = V^k Cov(g) [V^k]^T \quad (20)$$

These formulas can be made explicit for the case of the ML method. First, taking into account that the log likelihood function of the independent Poisson distributions, one obtains:

$$L(g|f) = \sum_i (g_i \log(\bar{g}_i) - \bar{g}_i - \log(\bar{g}_i!)) \quad (21)$$

The following explicit expressions can therefore be derived:

$$\nabla_x L(g|f) = H^T \text{diag}[Hf]^{-1} g - s \quad (22)$$

$$\nabla_{xx} L(g|f) = -H^T \text{diag}[Hf]^{-2} \text{diag}[g] H \quad (23)$$

$$\nabla_{xy} L(g|f) = -H^T \text{diag}[Hf]^{-1} \quad (24)$$

where  $s = P^T \mathbf{1}$  is a vector with all element equal to 1.

Taking into account also that for the ML algorithm the preconditioner is given by the relation:

$$\alpha C^k(f^k) = \text{diag}[f^k] \text{diag}[s^{-1}] \quad (25)$$

relations (17) and (18) become:

$$A^k = \text{diag}[\bar{f}^k] \text{diag}[s^{-1}] H^T \text{diag}[Hf]^{-2} \text{diag}[\bar{g} - \text{diag}[\bar{f}^{k+1}] \text{diag}[\bar{f}^k]^{-1}] + I \quad (26)$$

$$A^k = \text{diag}[\bar{f}^k] \text{diag}[s^{-1}] H^T \text{diag}[Hf]^{-1} \quad (27)$$

At this point, a second approximation can be introduced. It assumes a fast-enough convergence of the ML algorithm, which means that the projection of the current estimate is close to the noise-free projection. This approximation, used in [9] and [13], helps to simplify the expression of  $A^k$ :

$$A^k = \text{diag}[\bar{f}^k] \text{diag}[s^{-1}] H^T \text{diag}[Hf]^{-1} H \quad (28)$$

Summarizing, the image covariance can be calculated using Eq. 20, which relates the data noise to image uncertainties. The operator  $V$  is calculated at each iteration using the relations (19), (26) and (28).

The variances associated to each pixel can be represented as images, which allow correlating them with the reconstructed images.

#### 4. Analysis of phantoms for the optimization of the ML parameters

To properly assess the quality and uncertainties of the proposed tomographic inversion method, a systematic analysis with phantom emissions has been performed. The approach consists of performing the reconstructions with a series of known synthetic emissivity distributions and of evaluating the differences between the reconstructed 2D emissivity and the original one. To optimise the reconstructions, it is vital to properly select the smoothing factors. In particular, for the ML method, smoothness is introduced by means of the techniques described at the end of Section 2 (Eq. 8 and 9). Over/under-smoothing may lead to erroneous reconstruction of certain features. This problem can be overcome by scanning the smoothing parameters and selecting the ones, which minimize the differences between the two images (phantom and reconstruction). To this end, a systematic series of tomographic reconstructions have been performed for a comprehensive set of simulated emissivity distributions with shapes characteristic of JET bolometry. Two main cases, covering the most important types of emissivity for JET with the ILW, are shown in Figures 3 and 4. The emissivity of Figure 3 simulates a typical case in JET, with a strong emission of radiation in the divertor and around the X-point. The emission shown in Figure 4 is meant to represent what happens just after gas puffing

from a radial gas emission valve. The noised final profiles reported in Fig 3,4 have been computed adding first a normally generated random value of the 5% on the projections of the original phantoms. To better simulate the experimental situations the phantoms have also been generated over a background emission of an amplitude equal to 5% of the maximum value of the phantom themselves.

From the plots of figures 3 and 4, it is evident that the phantoms are well reconstructed. In particular, the experimental measurements, the projections, are almost perfectly reproduced. The total emitted power is also estimated with great accuracy. The discrepancy between the phantoms and the reconstructions is also typically within the uncertainties provided by the ML algorithm.

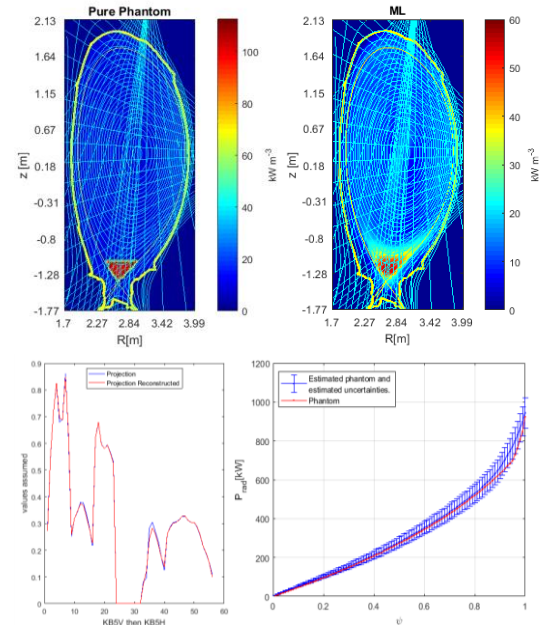
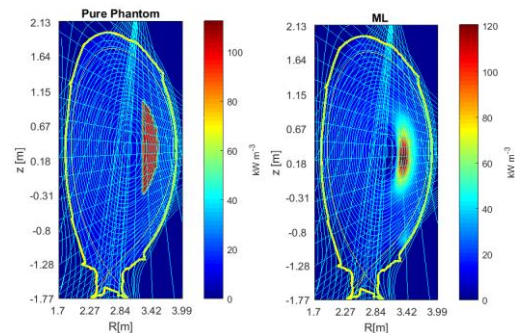


Figure 3 –Top left: phantom emissivity. Top right: reconstruction of the synthetic emissivity with the Maximum Likelihood code. Bottom left: synthetic and reconstructed projections. Bottom right:  $P_{\text{RAD}}$  versus the  $\psi$  coordinate with the estimate of the uncertainties in the emitted power as calculated by the analytic method described in Section 3. The uncertainties plotted are an average over 12 realisations of the noise.



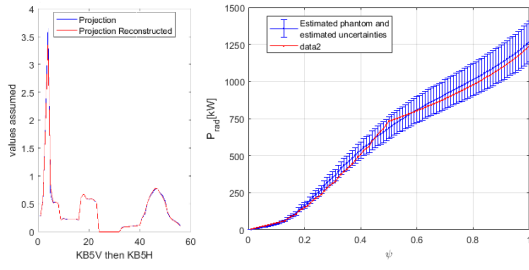


Figure 4 –Top left: phantom emissivity. Top right: reconstruction of the synthetic emissivity with the Maximum Likelihood code. Bottom left: synthetic and reconstructed projections. Bottom right:  $P_{RAD}$  versus the  $\psi$  coordinate with the estimate of the uncertainties in the emitted power as calculated by the analytic method described in Section 3. The uncertainties plotted are an average over 12 realisations of the noise.

## 5. Comparison with other inversion methods

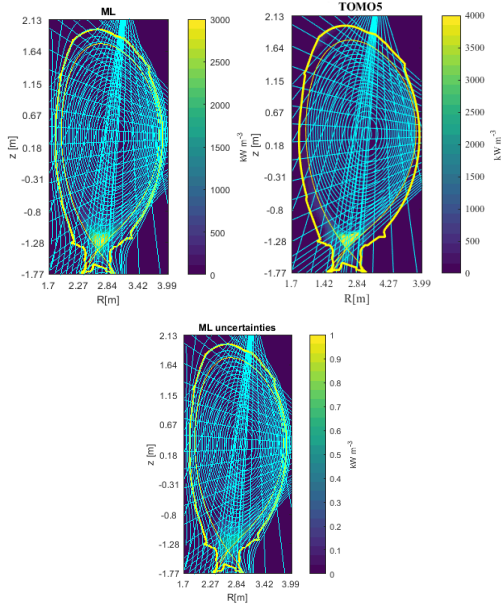


Figure 5– Shot number 84887 Top Left: reconstruction obtained with the method of the Maximum likelihood. Right: reconstruction obtained with TOMO5. Bottom: uncertainties estimation of the reconstruction from the ML method

An example of comparison between the reconstruction method proposed in this paper and the one typically use on JET, TOMO5, is provided for a time slice of discharge 84887 in Figure 5. The left hand side figure is the reconstruction obtained with the Maximum Likelihood and the other on the right with the traditional

program TOMO5 implementing Ingesson’s method [3]. In terms of macroscopic quantities, the difference between the two reconstructions is minimal. This can be appreciated inspection of Figure 6, which reports the evolution of the radiated power and the radiated fraction for the same discharge 84887. The differences between the two reconstructions never cause a discrepancy in the total radiated power exceeding 10%.

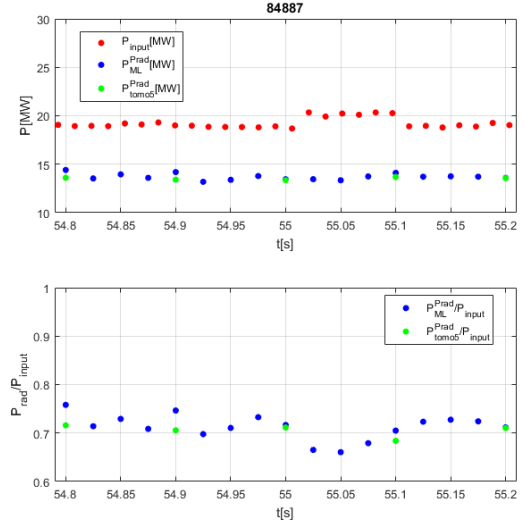


Figure 6– Shot number 84887. Time evolution of the total radiated power and the radiated fraction. The uncertainties plotted are an average over 12 realisations of the noise

## 6. Conclusions

The reconstruction technique based on the ML principle has been used to develop a methodology for the numerical evaluation of the statistical properties of the uncertainties in the tomographic remonstrations of JET bolometric measurements. The method is built on previous development techniques already deployed to perform tomographic inversions of the gamma ray and neutron emissions. The numerical tests with representative phantoms show that the method is able to provide good reconstructions in terms of shapes and resolution. In addition, the evaluation of the uncertainties is proved correct by a systematic analysis of the phantoms. Scanning the smoothing factors has allowed optimising this parameter for the various classes of emissivity detected in practice in JET plasmas. The excellent quality of the results is confirmed by the comparison with the method currently used routinely in JET.

As already discussed, the main advantage of the ML method is the possibility to evaluate the uncertainties accompanying the reconstruction and the calculated radiated power. This feature, together with the approach of the phantoms, permits to optimise the reconstructions parameters for the various experimental conditions. Moreover, the approach of combining an analytic estimate of the uncertainties with the phantoms provides a robust and principled method to address many experimental issues related to the diagnostic, such as the effect of the noise, of missing chords or the impact of the geometry on potential artefacts.

### Acknowledgments

This work has been carried out within the framework of the EUROfusion Consortium and has received funding from the Euratom research and training programme 2014-2018 under grant agreement No 633053. The views and opinions expressed herein do not necessarily reflect those of the European Commission.

### References

- [1] J. Wesson, Tokamaks, 4th Edn., Oxford University Press, 2011, ISBN: 9780199592234.
- [2] A. Huber, K. McCormick, P. Andrew, P. Beaumont, S. Dalley, J. Fink, J. C. Fuchs, K. Fullard, W. Fundamenski, L. C. Ingesson, F. Mast, S. Jachmich, G. F. Matthews, Ph. Mertens, V. Philipps, R. A. Pitts, S. Sanders, W. Zeidner, Upgraded bolometer system on JET for improved radiation measurements, *Fus. Eng. Des.* 82(5-14), 2007, 1327-1334.
- [3] L. C. Ingesson, B. Alper, H. Chen, A. W. Edwards, G. C. Fehmers, J. C. Fuchs, R. Giannella, R. D. Gill, L. Lauro-Taroni, M. Romanelli, Soft X-Ray Tomography During ELMs and Impurity Injection In JET, *Nucl. Fusion* 38, 1998, 1675-1694.
- [4] F. A. Matos, D. R. Ferreira, P. J. Carvalho, Deep learning for plasma tomography using the bolometer system at JET, *Fus. Eng. Des.* 114, 2017, 18-25.
- [5] O. Barana, A. Murari, P. Franz, L. C. Ingesson, G. Manduchi, Neural networks for real time determination of radiated power in JET, *Rev. Sci. Instrum.* 73-5, 2002, 2038-2043.
- [6] T. Craciunescu, G. Bonheure, V. Kiptily, A. Murari, I. Tiseanu, V. Zoita., The Maximum Likelihood Reconstruction Method for JET Neutron Tomography, *Nucl. Instrum. Meth. A*, 595, 2008, 623-630.
- [7] T. Craciunescu, G. Bonheure, V. Kiptily, A. Murari, I. Tiseanu, V. Zoita, A Comparison of Four Reconstruction Methods for JET Neutron and Gamma Tomography, *Nuclear Instruments & Methods in Physics Research Section A* 605, 2009, 373-384.
- [8] T. Craciunescu, A. Murari, V. Kiptily, I. Lupelli, A. Fernandes, S. Sharapov, I. Tiseanu, V. Zoita., Evaluation of reconstruction errors and identification of artefacts for JET gamma and neutron tomography, *Review of Scientific Instruments* 87, 2016, 013502.
- [9] H. H. Barrett, D. W. Wilson, B. M. W. Tsui, Noise properties of the EM algorithm: I. Theory, *Phys. Med. Biol.* 39, 833-346 (1994).
- [10] W. Wang, G. Gindi, Noise analysis of MAP-EM algorithms for emission tomography *Phys. Med. Biol.* 42, 2215-32 (1997).
- [11] E. J. Soares, C. L. Byrne, S. J. Glick, Noise characterization of block-iterative reconstruction algorithms: I. Theory *IEEE Trans. Med. Imaging* 19, 261-70 (2000).
- [12] E. J. Soares, S. J. Glick, J. W. Hoppin, Noise characterization of block-iterative reconstruction algorithms: II. Monte Carlo simulations *IEEE Trans. Med. Imaging* 24, 112-21 (2005).
- [13] J. Qi, A unified noise analysis for iterative image estimation *Phys. Med. Biol.* 48, 3505-19 (2003).
- [14] J. A. Fessler, W. L. Rogers, Spatial resolution properties of penalized-likelihood image reconstruction: space invariant tomographs *IEEE Trans. Image Process.* 5, 1346-58 (1996).
- [15] A. Teymurazyan, H. S. Jans, T. Riauka, D. Robinson, Properties of Noise in Positron Emission Tomography Images Reconstructed with Filtered-Backprojection and Row-Action Maximum Likelihood Algorithm, *Journal of Digital Imaging* 26-3 (2012) 447-56.
- [16] A. A. Sanchez, Estimation of noise properties for TV-regularized image reconstruction in computed tomography, *Phys. Med. Biol.* 21-60 (2015) 7007-33.
- [17] R. Kueng, B. Driscoll, P. Manser, M. K. Fix, M. Stampanoni, H. Keller, Quantification of local image noise variation in PET images for standardization of noise-dependent analysis metrics, *Biomedical Physics & Engineering Express*, 3-2 (2017) 025007.

- [18] K. Lange, R. Carson, EM reconstruction algorithms for emission and transmission tomography, J Comput. Assist. Tomogr. 8 (2), 306-16 (1984).